Journal of Engineering Science and Technology
Special Issue on Applied Engineering and Sciences, October (2014) 51 - 65

A COMBINED THEORETICAL AND EXPERIMENTAL APPROACHES TOWARDS DESIGNING NIR DYES FOR DYE-SENSITISED SOLAR CELLS

Y. YAMAGUCHI[1], S. S. PANDEY[2,*],
N. FUJIKAWA[2], Y. OGOMI[2], S. HAYASE[2]

[1]Nippon Steel & Sumikin Chemical Company Limited, 46-80, Nakabaru, Sakinohama, Tobata, Kitakyushu 804-8503, Japan
[2]Graduate School of LSSE, Kyushu Institute of Technology, 2-4, Hibikino, Wakamatsu, Kitakyushu 808-0196, Japan
*Corresponding Author: shyam@life.kyutech.ac.jp

Abstract

Sensitizing dyes especially having capability of sharp light absorption in the near infrared region play a pivotal role towards enhancing the photovoltaic efficiency of dye-sensitised solar cells. Effort has been directed towards the optimization of suitable calculation parameters for the theoretical calculations to assist the design of novel sensitizers for the dye-sensitised solar cells using Gaussian program package. Suitability of the calculation parameters as well as calculated results using the same model, unsymmetrical squaraine dye (SQ-1) was designed, synthesized and used for their characterisation and photovoltaic applications. Calculation results were performed in both ground and excited states of this molecule and indicate that B3LYP and B3PW91 are quite suitable hybrid functional for theoretical calculation using DFT and 6-311G basis set. Electronic absorption maximum for SQ-A in ethanol solution exhibits the peak at 650 nm which was found to be only 47 nm (0.04 eV) higher as compared to the calculated value (603 nm) using PCM solvent model under TD-DFT.

Keywords: MO calculation, Gaussian, Squaraine dye, NIR sensitization, Dye-sensitized solar cells.

1. Introduction

Dye-sensitized solar cells (DSSCs) are currently being intensively investigated as a promising photovoltaic cell owing to its unique operating mechanism along with the ecological and economical fabrication. Impressive photo-conversion efficiency over 10% has been demonstrated by the design and development of potential organic as

Nomenclatures

B3LYP	Becke 3 parameter exchange functional with correlation functional by Lee, Yang and Parr
B3PW91	Becke 3 parameter exchange functional with Perdew and Wang's 1991 gradient-corrected correlation functional
BPV86	Burke and Perdew's 1986 functional with correlation replaced by Vosko et al. [28].
Eg	Optical band gap
HCTH	Handy's family of functionals including gradient-corrected correlation
Jsc	Short circuit current density
MP2	Moller-Plesset second order correlation energy correction
MP4	Moller-Plesset fourth order correlation energy correction
MPW	Modified Perdew and Wang's 1991 gradient-corrected correlation functional
PBE	The 1996 exchange functional of Perdew, Burke and Ernzerhof
QCSID	Quadratic Configuration Interaction with Single and Double Excitation
TD-DFT	Time-Dependent Density Functional Theory
THCTH	The τ-dependent member of the HCTH family of functional
TPSS	The τ-dependent gradient-corrected functional of Tao, Perdew, Staroverov, and Scuseria
Voc	Open circuit voltage

Abbreviations

AM1	Austin Model 1
CB	Conduction Band
CDCA	Chenodeoxycholic Acid
CI	Configuration Interaction
DSSC	Dye-Sensitized Solar Cells
FAB-MS	Fast Ion Bombardment Mass Spectroscopy
FF	Fill factor
HF	Hartree-Fock
HOMO	Highest Occupied Molecular Orbital
HPLC	High Performance Liquid Chromatography
IPCE	Incident photon to current conversion efficiency
LSDA	Local Spin Density Approximation
LUMO	Lowest Unoccupied Molecular Orbital
MALDI -TOF	Matrix Assisted Laser Desorption and Ionization Time-of-Flight
MNDO	Modified Neglect of Differential Overlap
NIR	Near Infra-Red
NMR	Nuclear Magnetic Resonance
PCM	Polarization Continuum Model
PM3	Parametric Model 3
STO	Slator Type Orbitals

well as inorganic sensitizers which harvest photon effectively in the visible region of the wavelength [1, 2]. Attainment of nearly quantitative photon harvesting by

these visible sensitizers in the case of DSSCs based on nanoporous TiO_2 and potential iodine and cobalt based redox electrolytes indicates the highly efficient photogeneration, charge injection and charge collections [3, 4]. Lack of effective photon harvesting beyond the 750 nm offers a bottle-neck towards the achievable photo-conversion efficiency. This gives a hope for the development of novel sensitizers capable of efficient light absorption and photon harvesting in near infra-red (NIR) wavelength region. In the recent past, efforts have been made to develop single sensitizer capable of photon harvesting in wide wavelength region encompassing from visible to IR but results were not encouraging. Actually enhancing the photosensitivity in far-red to IR wavelength region led to decreased photon harvesting in the visible region leading to decreased overall photo-conversion efficiency [5, 6]. To circumvent this problem, concept of dye cocktail using two or more dyes for the simultaneous sensitization of wide band gap semiconductor and synergistic photon harvesting by sensitizers was proposed and experimentally verified by many research groups [7, 8]. In the hybrid DSSCs based on fabrication of photo-anode from a dye cocktail it quite often led to hampered photon harvesting due to inter-dye unfavourable interactions [9, 10]. This problem was solved by adopting the fabrication of photo-anode using the dye bilayer/multilayer architecture, where such unfavourable interactions were minimized leading to enhanced photo-conversion efficiency [11-13].

A suitable dye for its application in DSSCs should (a) have high molar extinction coefficients, (b) possess a suitable anchoring group, (c) energy in its highest occupied molecular orbitals (HOMO) should be lower than energy level of redox electrolyte or hole conductor and (d) energy of the lowest unoccupied molecular orbital (LUMO) must be higher than that of wide band gap semiconductor. Since structural possibility for designing dye molecules are huge, therefore, theoretical predictions pertaining to the calculation of HOMO and LUMO energy level along with the electronic absorption spectra are expected to accelerate the dye development research. In this article, electronic structure calculations in ground and excited state were conducted using Gaussian G09 program package. The aim was to optimise the calculation parameters which can predict the results of energetics as well as electronic absorption spectra closer to the experimentally observed values. For this purpose, we selected a model unsymmetrical squaraine dye molecule (SQ-A) having molecular structure shown in Fig. 1. In parallel, this compound was also synthesized, characterised and used for the fabrication of DSSC. Calculated results pertaining to the energetics, band gap and absorption maximum were then compared with experimentally observed values to find the optimum parameters for the theoretical calculations.

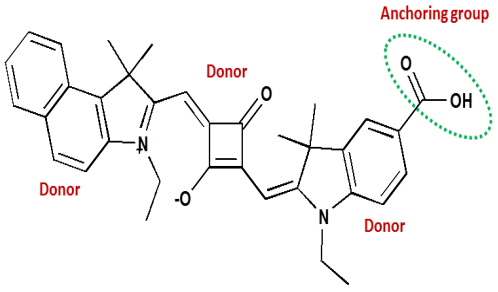

Fig. 1. Chemical Structure of Model Unsymmetrical Squaraine Dye SQ-A.

2. Experimental

2.1. Materials, instruments and methods

Synthesized squaraine dye (SQ-A) and dye intermediates were analysed by high performance liquid chromatography (HPLC) for monitoring the reaction progress and final purity of the compound. Mass of the intermediates as well as final SQ dyes were confirmed by MALDI-TOF-mass (Applied Bio-systems) or fast ion bombardment (FAB) mass in positive ion monitoring mode. Nuclear magnetic resonance (NMR) spectra were recorded on a JEOL JNM A500 MHz spectrometer in $CDCl_3$ or d_6-DMSO with reference to TMS for structural elucidation. Electronic absorption spectroscopic investigations were made by UV-visible spectrophotometer (JASCO V 550). HOMO energy level of the squaraine dye was determined by photoelectron spectroscopy in air (PESA model AC3) from Riken Keiki Co. Ltd. Japan while the LUMO energy level was determined from the edge of optical absorption using electronic absorption spectroscopy considering it as Eg using the relation LUMO = HOMO + Eg.

2.2. Synthesis of SQ-A and its intermediates

Aromatic ring carboxy functionalised indole derivative 2,3,3-trimethyl-*3H*-indole-5-carboxylic acid and intermediate **5** was synthesized and characterised as per our previous publications following the methodology reported by Pham et al. [14, 15]. Sensitizing dye SQ-A and corresponding dye intermediates have been synthesized as per the scheme shown in Fig. 2.

2.2.1. Synthesis of 2, 3, 3-trimethyl-1-Ethyl-Benz[e]indolium iodide [2]

5.0 gm (24 mmol) of 2,3,3-trimethyl-Benz[e]indole and 5.5 gm (36 mmol) of 1-Iodoethane were dissolved in 200 ml of dehydrated acetonitrile and reaction mixture was refluxed for 96 hours under nitrogen. After completion of the reaction, solvent was evaporated and the crude product was washed with ample diethyl ether giving 8.7 gm of titled compound as whitish powder in 99% yield having 99% purity as confirmed by HPLC. TOF-mass (measured 238.0; calculated 238.6) confirms the successful synthesis of this compound.

2.2.2. Synthesis of 3-Butoxy-4-[(1-Ethyl-1,3-dihydro-3,3-dimethyl-2H-Benzindole-2-ylidene) methyl]-3-cyclobutene-1,2-dione [3]

In a round bottom flask fitted with condenser, 1.82 gm (5 mmol) of 2,3,3-trimethyl-1-ethyl-4,5 benzo[e]indolium iodide [2], 1.12 gm (5 mmol) of 3,4-dibutoxy-3-cyclobutene-1,2-dione, 1.0 ml of Triethylamine were dissolved in 10 ml of dehydrated butanol. Reaction mixture was heated at 70^{o}C for 2 hours leading to green solution. Solvent was removed at rotary evaporator and product was purified by column chromatography (silica gel) with ethyl acetate and hexane as eluent giving 1.34 gm (3.44 mmol) of titled compound in 69% yield and 99% purity as confirmed by HPLC. Compound was confirmed by MALDI-TOF mass [calculated 389.10 and measured 389.52].

2.2.3. Synthesis of unsymmetrical squaraine dye SQ-A (6)

Unsymmetrical squaraine dye SQ-A was synthesized using semi-squaraine ester after hydrolysis (4) and compound (5) as follows: In a round bottom flask fitted with condenser, 1.0 gm (2.17 mmol) of compound (4) and 780 mg (2.17 mmol) of compound (5) and 40 ml of 1-butanol: benzene mixture (1:1, v/v) were added. Reaction mixture was refluxed for 12 hours using Dean-Stark trap. Reaction mixture was cooled, solvent was evaporated and product was purified by silica gel column chromatography using chloroform: methanol as eluting solvent. 630 mg of final titled compound (6) was obtained as a blue solid in 99% purity as confirmed by HPLC and 55% yield. MALDI-TOF-mass (calculated 546.25 and observed 547.46, M^+H) confirms the successful synthesis of the unsymmetrical squaraine dye SQ-A.

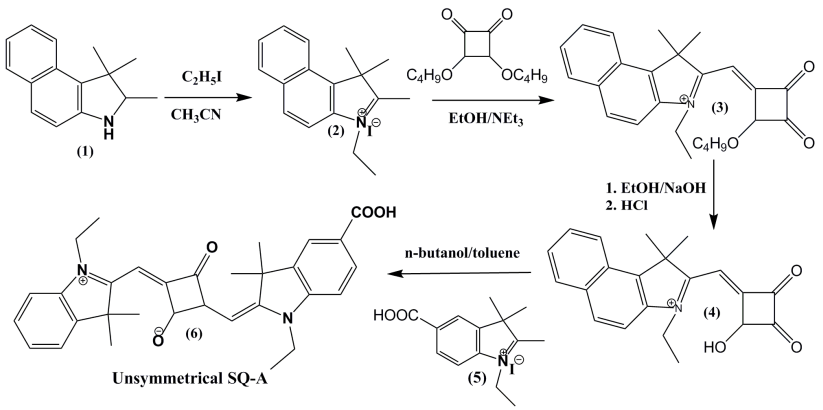

Fig. 2. Synthetic Scheme for Unsymmetrical Squaraine Dye SQ-A).

2.3. DSSC fabrication and characterisation

DSSCs were fabricated using Ti-Nanoxide D/SP paste (Solaronix SA) which was coated on a Low E glass (Nippon Sheet Glass Co., Ltd.) by a doctor-blade. The substrate was then baked at 450°C to fabricate TiO_2 layers of about 12-13 μm thickness. This nanoporous TiO_2 layer was subjected to surface treatment by 40 mM aqueous solution of $TiCl_4$ at 70°C for 2 hours followed by its baking at 450°C for 30 min. The substrate was dipped in the solution containing dye in the presence of dye de-aggregating agent chenodeoxycholic acid (CDCA) for the adsorption of dye on to the nanoporous TiO_2 layer. The dye concentration was fixed to be 0.25 mM while CDCA concentration was 2.5 mM. A Pt sputtered SnO_2/F layered glass substrate was employed as the counter electrode. Electrolyte (WWS30) containing LiI (500 mM), Iodine (50 mM), t-butylpyridine (580 mM), MeEtIm-DCA (ethylmethylimidazolium dicyanoimide)(4:6 wt/wt) (600 mM) in acetonitrile, was used to fabricate the DSSC. A Himilan film (Mitsui-DuPont Poly-chemical Co., Ltd.) of 25 μm thickness was used as a spacer. The cell area was 0.2025 cm^2 defined precisely by metal mask. Solar cell performance was measured with a solar simulator (CEP-2000, Bunko Keiki, Japan) equipped with Xenon lamp for the light exposure. The spectrum of the solar simulator and its

power were adjusted to be at global air mass 1.5 condition (100 mW/cm^2) using a spectroradiometer (LS-100, Eiko Seiki, Japan).

3. Theoretical Calculation

Theoretical calculations pertaining to the structural optimisation as well as electronic absorption spectra for the squaraine dye (SQ-A) was conducted on Dell work-station using Gaussian G09 program package [16]. Calculation was done in both of the isolated molecule in gaseous state as well as in solution in the framework of the self-consistent reaction field polarizable continuum model (PCM) [17] using ethanol solvent. Previous theoretical investigations also emphasize that incorporation of solvent effects is necessary to describe the electronic absorption spectra more accurately [18]. In the theoretical calculations, judicious selection of a suitable basis set, theory and functional are required to make a logical balance between the computation cost and accuracy. In this work, 6-311G basis set was utilized with TD-DFT for electronic structure calculations. In the Gaussian program package, one has to define the calculation parameters like basis set, theory as well as suitable functional. Under the DFT, there are various functional like LSDA, BPV86, B3LYP, B3PW91, MPW1PW91, PBEPBE, HCTH, THCTH, TPSSTPSS, etc. Calculation was performed to optimise the structure using all of these functional to ascertain the most optimum functional.

4. Results and Discussion

4.1. Electronic absorption spectrum

SQ-A shows the absorption maximum (λ_{max}) at 648 nm having very high molar extinction coefficient ($\varepsilon = 2.4\times10^5$ dm^3.mol^{-1}.cm^{-1}) with narrow full width at half maximum (FWHM) of 30 nm. The observed λ_{max} at 648 nm is associated with π-π^* electronic transition originating from electronic transition from the HOMO to the LUMO of the dye. At the same time it also exhibits a small shoulder at 610 nm which could be attributed to the high energy vibronic transition [19]. In solution state, although it is not much pronounced but upon adsorption on to the nano-porous TiO_2 it becomes pronounced due to enhanced intermolecular interaction and is indicative of dye aggregation. Considering it as a marker, Yum et al. [20] have reported that the ratio of optical density of the aggregate band (low wavelength shoulder) and the monomer band (λ_{max}) can be visualized as indicator of the dye aggregation. Increase in this ratio exhibits the enhanced H-aggregation. They have also experimentally demonstrated that use of CDCA led to the decrease in this ratio indicating the suppression of dye aggregation.

4.2. Energy band diagram

Design of a novel sensitizer for DSSC application is based on the judicious control of energy level of HOMO and LUMO with respect to the energy level of the redox couple (I^-/I_3^-) and conduction band (CB) of TiO_2, respectively.

The energy band diagram of the unsymmetrical squaraine dye SQ-A along with the energy level of the TiO_2 and I^-/I_3^- redox couple has been shown in Fig. 3. Redox potential of I_3^-/I^- redox couple - 4.9 eV and CB of TiO_2 - 4.0 eV were taken from the reported literatures [21, 22]. To construct this energy diagram, the HOMO energy level of the dye was estimated from PESA which was found to be –5.14 eV. At the same time LUMO energy level was estimated by adding energy corresponding to the Eg of the dye to the HOMO energy level. Eg was estimated from the onset of the optical absorption edge as shown in Fig. 4 which comes to be 675 nm (1.84 eV). Thus the LUMO energy level of the dye was estimated to be -3.30 eV. It has been reported that an energy barrier > 0.2 eV necessary for facile electron injection and dye regeneration in DSSC [23]. A perusal of Fig. 3 clearly corroborates that in the case of SQ-A dye the driving force for electron injection and dye regeneration is 0.70 eV and 0.23 eV, respectively which ensures it's functioning as sensitizer for the DSSC.

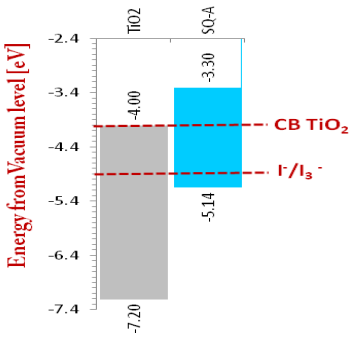

Fig. 3. Electronic Absorption Spectrum of SQ-A in Ethanol Solution (10 μM). Inset Shows the Ethanolic Solution of the Dye.

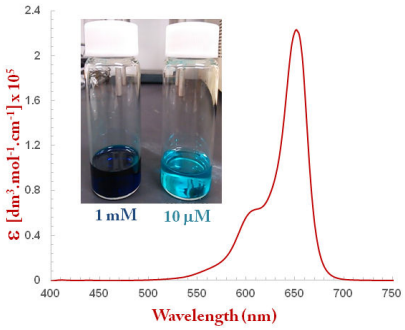

Fig. 4. Energy Band Diagram for Unsymmetrical Squaraine Dye Along with the TiO_2 and Iodine Based Redox Electrolyte.

4.3. Photovoltaic characteristics

Current–voltage (I–V) characteristics of DSSCs based on dye (SQ-A) under standard global AM 1.5 solar irradiation has been shown in Fig. 5(a). For the reproducibility of the observed results, three DSSCs were independently fabricated under the identical experimental conditions. Photovoltaic parameters deduced from the I-V characteristics are shown in the Table 1. A perusal of Fig. 5 and Table 1 clearly indicates the reproducibility of the measured results. Amongst the three DSSCs, best performance was obtained for the device-1 giving short circuit current density (Jsc) of 10.27 mA/cm^2, open circuit voltage (Voc) of 0.66 V, fill factor (FF) of 0.62 leading to the overall power conversion efficiency of 4.18%. Very small standard deviations amongst device parameters further validate the good reproducibility of the experimental results. In order to elucidate the observed Jsc and investigate the photon harvesting behaviour, photo-current action spectra for the DSSCs fabricated with SQ-A was also measured and shown in Fig. 5(b). Photocurrent action spectrum is basically the variation

of incident photon to current conversion efficiency (IPCE) as a function of wavelength after the monochromatic light illumination. A perusal of this figure clearly corroborates that the action spectrum is perfectly symbatic (nearly similar shape and peak maximum) with the absorption spectrum shown in Fig. 4 with spectral broadening due to aggregate formation in solid-state. The maxima of the IPCE observed for different devices are nearly similar and in accordance with observed Jsc values.

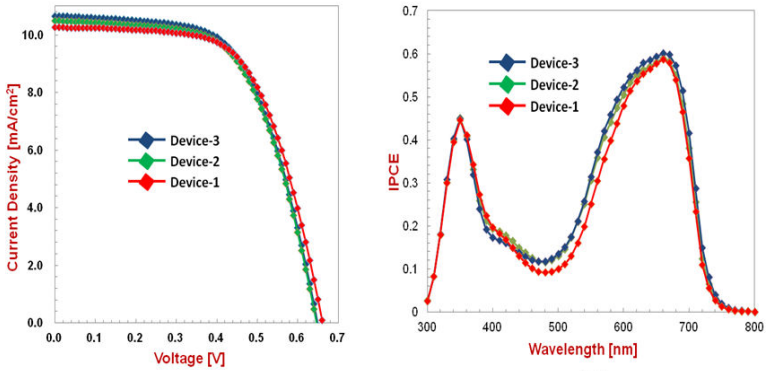

Fig. 5. I-V Characteristics of DSSCs Fabricated Using SQ-A under 100 mW/cm^2 Simulated Solar Irradiation (a) and Photocurrent Action Spectra of the Same after Monochromatic Light Illumination (b).

Table 1. Photovoltaic Parameters for the DSSCs Fabricated Using SQ-A Under Identical Experimental Conditions. Values Shown in the Parentheses Indicate the Standard Deviations Amongst the Observed Results.

Device parameters	Device-1	Devic-2	Device-3	Average
Efficiency (%)	4.18	4.09	4.15	4.14 (± 0.05)
FF	0.62	0.60	0.60	0.61 (± 0.01)
Voc (V)	0.66	0.65	0.65	0.65 (± 0.006)
Jsc (mA/cm^2)	10.27	10.49	10.65	10.47 (± 0.19)

5. Theoretical Investigations

5.1. Structural optimization and MO calculations

The main aim of MO calculation lies in the accurate prediction of the properties and many calculation techniques and methodologies have been developed. Such techniques are being widely used considering the computational cost and accuracy which are inversely proportional. Various semi-empirical and ab-initio methods have been developed to achieve this goal. The ab-initio methods of electronic structure calculations have both pros and cons. It does not need any experimental parameters and is relatively more accurate but it needs the high computational cost as compared to semi-empirical methods like AM1, PM3 and

MNDO, etc. Amongst the various ab-initio methods, the accuracy and computation cost depends on the adopted calculation methodologies which are in the order of (HF) < MP2 < MP4 < QCISD <<< Full CI. At the same time, judicious selection of a suitable basis set which is approximate representation of atomic orbitals and is equally important to make a logical balance between the computation cost and accuracy of calculated results. Amongst electronic structure calculation methodologies, DFT has emerged as one of the reliable methods for the theoretical treatment and suitability of dye molecular structure as a photosensitizer. DFT considers the electron and lone pair correlations like ab-initio methods but only at the computational cost of HF. Its time dependent extension (TD-DFT) has been demonstrated to provide reliable values for the excitation energies with the standard correlation functional which has been extensively used for the design and development of new dyes for the DSSCs [24].

To get the further insight, ground state electronic structure calculation pertaining to the structural optimization in gaseous state was performed for the SQ-A using Gaussian G09. Structural optimization was conducted using diffuse basis set (6-311G) and applying the DFT and most commonly employed hybrid functional (B3LYP). Results of the calculation in terms the optimized minimum energy structure along with the electronic distribution in HOMO and LUMO are shown in Fig. 6 and Table 2. A perusal of Fig. 6 clearly reveals that electron density in HOMO is mainly centralised at squaraine core which is associated with the π-framework of the dye. On the other hand, electron density distribution in LUMO associated with π^* MO is also delocalised over the entire molecular framework with reduction of electron density at squaric acid core and sufficient diversion of electron density at the –COOH anchoring group present in the indole ring. Such a diversion indicates the sufficient electronic coupling to be accomplished when this dye is attached to the oxide semiconductor leading to the facile electron injection upon the photoexcitation.

It can be seen from the calculation results (Table 2) that utilization of solvent ethanol in calculation using PCM model there is a downward shift in the energy level without having appreciable impact on the band gap estimated from the difference in the energy level of HOMO and LUMO. In fact inclusion of the solvent molecules in the electronic structure calculation takes the system nearer to the real environment bridging the error gap in the theoretical calculation and experimental results. In the theoretical investigations pertaining to Ru and Os based sensitizers, Gullemoles et al. [25] have also advocated that inclusion of solvents effects is necessary and gives relatively better results. In the present work also calculation conducted for far-red sensitizing dye SQ-A clearly reveals that utilization of ethanol solvent in the PCM model rather gives better result and calculated energies of the HOMO and LUMO exhibit the better agreement with the experimentally observed values.

Table 2. Calculated Results after the Structural Optimisation with 6-311G Basis Set and B3LYP Functional under DFT Along with the Experimental Results.

Parameters	Gaseous State	Ethanol solvent	Experimental
HOMO (eV)	- 4.89	- 5.06	- 5.14
LUMO (eV)	- 2.77	- 2.91	- 3.30
Eg (eV)	2.12	2.15	1.84

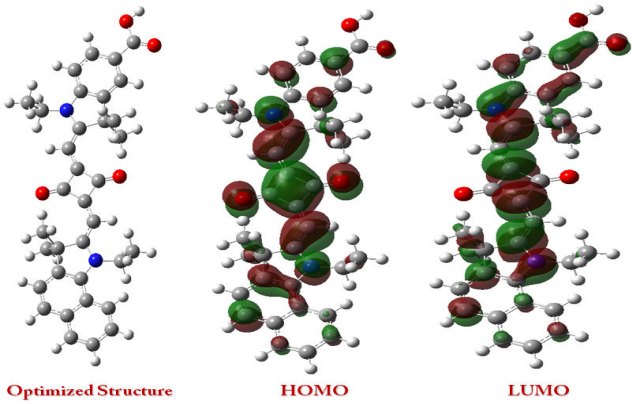

Fig. 6. Calculated Stereograph (Optimised Structure), HOMO and LUMO for SQ-A.

5.2. Calculations for electronic absorption spectra

After optimization of geometry for **SQ-A**, electronic structure calculation using TD-DFT was also performed at B3LYP/6-311G level of theory in order to calculate the excitation energies at the optimised geometries for the ground state and lowest singlet excited states. This calculation was performed both of the isolated molecule in gaseous state as well as in ethanol solution using PCM model in order to simulate the electronic absorption spectra.

Excited state TD-DFT calculations provide information about the electronic transitions, molar extinction coefficients and oscillator strength which is shown in Fig. 7. Absorption spectrum for the isolated gaseous state exhibits intense electronic transition at 580 nm having oscillator strength of 1.6061 associated with main π-π* electronic transition from the HOMO-LUMO. At the same time in the solution this has been found to be red-shifted to 603 nm having relatively enhanced oscillator strength of 1.9425. A perusal of this calculated λ_{max} of 603 nm which is slightly blue-shifted with the experimental one (650 nm) in the same solvent exhibiting only a difference of 0.04 eV between the experimental result and theoretical calculation indicating potentiality of such methodology towards the theoretical prediction of absorption spectra for the design and development of novel NIR sensitizers.

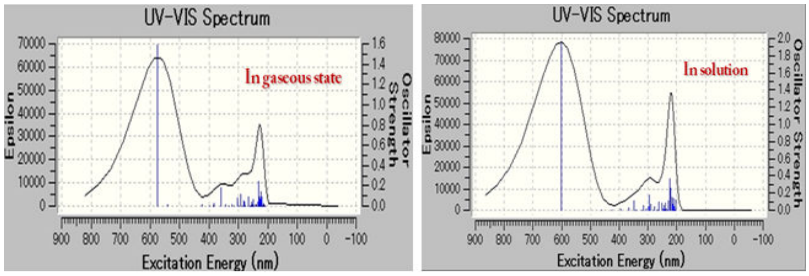

Fig. 7. Simulated Electronic Absorption Spectra of SQ-A in Gaseous State and Ethanol Solution.

5.3. Effect of different functionals under TD-DFT calculation

TD-DFT calculation platform has been extensively investigated for the design and development of novel sensitizers along with the judgment for their suitability as sensitizer for DSSC applications. In the Gaussian program package under DFT, there is a provision for several functionals to incorporate during the calculation after specifying the suitable basis set. There are various kinds of functional such as exchange functional, correlation functional, standalone functionals, hybrid functionals, and long range corrected functionals. The three parameter exchange functional of Becke and correlation functional of Lee, Yang and Parr (B3LYP) [26] has been most widely used for the ground state geometry optimisation as well as electronic absorption spectral calculation by material scientist community. Apart from this functional, several other functionals like PBE, MPW1 and BPW91 [27] have also been used for the calculation of organic sensitizers for DSSCs mainly visible light absorbing dyes. Efforts have been made to calculate the HOMO and LUMO energy along with the electronic absorption spectra for SQ-A using different functionals like B3LYP, B3PW91, MPW1, LSDA, BPV86, PBE, PBE1, THCTH, HCTH and TPSS available under DFT method in Gaussian G09 using 6-311G basis set.

Figure 8 exhibits the calculated electronic absorption spectra of SQ-A in gaseous state under TD-DFT/6-311G level of theory using different functional. A perusal of this figure reveals a strong peak in the range of 400-800 nm associated with HOMO-LUMO electronic transition. The behavior is very similar to that observed with experimental data in solution and position of the λ_{max} was found to be affected by the selection of functional considered during the theoretical calculation. In terms of observed behavior it can be seen that functional like MPW1, PBE1, B3PW91 and B3LYP exhibits relatively blue-shifted λ_{max} as compared to other functional leading to increased gap between calculated results and experimental value observed at 650 nm in the ethanol solution. The details of the calculated results on energetics and electronic absorption spectra are shown in Table 3.

It is interesting to see from Table 3 that calculation results pertaining to the utilization of different functional under same level of theory give variable results in terms of the energies of the HOMO and LUMO along with λ_{max} values. Therefore, we have to make a selection that whether we are interested in the calculation of energetics or the electronic absorption spectra. For example functional like HCTH and PBE gives the calculated λ_{max} values of 635-640 nm which is very near to the experimentally observed λ_{max} of 650 nm in solution. On the other hand the calculated value of HOMO of about – 4.4 eV is far from the experimentally observed value of – 5.14 eV. At the same time, the energy of the HOMO-LUMO gap (about 1.2 eV) is also too much different from the experimentally determined optical band gap of 1.84 eV. Although HOMO energy level (-5.11 eV) and λ_{max} (629 nm) calculated using functional LSDA are very close to the experimental values (-5.14 eV) and 650 nm respectively, its LUMO energy is too much stabilised giving the too small HOMO-LUMO gap of 1.24 eV. Considering all of these pros and cons, B3LYP and B3PW91 functional give rather more reliable results pertaining to the energetics, HOMO-LUMO gap as well as λ_{max} for the **SQ-A** dye.

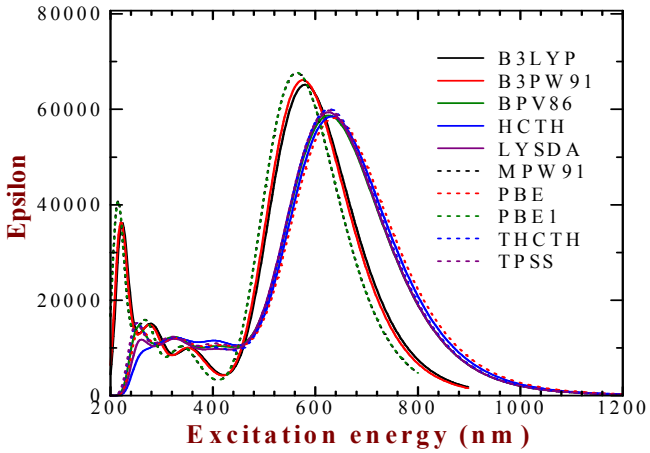

Fig. 8. Simulated Electronic Absorption Spectra of SQ-A in Isolated Gaseous State Using Different Functionals Under TD-DFT Calculation.

Table 3. Calculated HOMO and LUMO Energies Along with Electronic Absorption Spectral Parameters for SQ-A Utilising Different Functionals Under TD-DFT Level of Theory and 6-311G Basis Set.

Functionals	HOMO (eV)	LUMO (eV)	Band gap (eV)	λ_{max} (nm)	Oscillator Strength
MPW1PW91	- 5.04	- 2.67	2.37 (523 nm)	563	1.6692
PBE1PBE1	- 5.02	- 2.67	2.35 (528 nm)	564	1.6707
B3PW91	- 4.83	- 2.81	2.02 (613 nm)	576	1.6290
B3LYP	- 4.89	- 2.77	2.12 (584 nm)	580	1.6061
TPSSTPSS	- 4.36	- 3.10	1.26 (984 nm)	628	1.4870
LSDA	- 5.11	- 3.87	1.24 (1000 nm)	629	1.4449
BPV86	- 4.47	- 3.23	1.24 (1000 nm)	629	1.4290
THCTH	- 4.52	- 3.27	1.25 (992 nm)	629	1.4653
HCTH	- 4. 46	- 3.24	1.22 (1016 nm)	635	1.4260
PBEPBE	- 4.40	- 3.18	1.22 (1016 nm)	640	1.4155

(*Values shown in the parentheses indicate the wavelength corresponding to the HOMO-LUMO energy gap.*)

6. Conclusions

A combined theoretical and experimental approach has been implemented to design and develop NIR dyes for the DSSCs. As a model compound, far-red sensitive unsymmetrical squaraine dye (SQ-A) was designed, synthesized and used as sensitizer for DSSC along with the theoretical investigations. Under simulated solar irradiation at AM 1.5 condition, this dye exhibits average external power conversion efficiency of 4.14% and maximum IPCE of 60% at its absorption maximum. It has been found that implementation of PCM solvent model in calculation at TD-DFT/B3LYP platform leads to the 23 nm bathochromic shifts in the electronic

absorption maximum as compared to gaseous state leading to very good match between experimental and calculated values with difference of only 0.04 eV. Theoretical calculation pertaining to the TD-DFT and 6-311G basis set are found be good balance between the computational cost and accuracy between calculated and experimental result. Under TD-DFT, choice of the suitable functional should be made considering the whether we are interested in the electronic absorption spectra, energetics or both. In general, B3LYP and B3PW91 functional are found to be relatively better to give satisfactory results pertaining to the energetics as well as electronic absorption spectra.

References

1. Gratzel, M. (2005). Solar energy conversion by dye-sensitised photovoltaic cells. *Inorganic Chemistry*, 44(20), 6841-6851.
2. Bessho, T.; Zakheeruddin, S.M.; Yeh, C.Y.; Diau, E.W.G.; and Gratzel, M. (2010). Highly efficient mesoscopic dye-sensitised solar cells based on donor-acceptor-substituted porphyrins. *Angewandte Chemi International Edition*, 39, 49(37), 6646- 6649.
3. Yella, A.; Lee, H.W.; Tsao, H.N.; Yi, C.; Chandiran, A.K.; Nazeeruddin, M.K.; Diau, E.W.G.; Yeh, C.Y.; Zakheeruddin, S.M.; and Gratzel M. (2011). Porphyrin-sensitised solar cells with cobalt (II/III)-based redox electrolyte exceed 12% efficiency. *Science*, 334, 629-634.
4. Gao, F.; Wang, Y.; Shi, D.; Zhang, J.; Wang, M.; Jing, X.; Baker, R.H.; Wang, P.; Zakheeruddin, S.M.; and Gratzel, M. (2008); Enhance the optical absorptivity of nanocrystalline TiO_2 film with high molar extinction coefficient ruthenium sensitisers for high performance dye-sensitised solar cells. *Journal of American Chemical Society,* 130(32), 10720-10728.
5. Tian, H.; Yang, X.; Chen, R.; Hagfeldt, A.; and Sun, L. (2008). A metal-free black dye for panchromatic dye-sensitised solar cells. *Energy and Environmental Science*, 2, 674-677.
6. Altobello, S.; Argazzi, R.; Caramori, S.; Contado, C.; Da-Fre, S.; Rubino, P.; Chone, C.; Larramona, G.; and Bignozzi, C.A. (2005). Sensitisation of Nanocrystalline TiO2 with black absorbers based on Os and Ru Polypyridine complexes. *Journal of American Chemical Society,* 127(44), 15342-15343.
7. Chen, Y.S.; Zeng, Z.H.; Li, C.; Wang, W.B.; Wang, X.S.; and Zhang, B.W (2005). Highly efficient co-sensitisation of nanocrystalline TiO_2 electrodes with plural organic dyes. *New Journal of Chemistry*, 29(6), 773-776.
8. Guo, M.; Diao, P.; Ren, Y.J.; Meng, F.; Tian, H.; and Kai, S.M. (2005). Photo-electrochemical studies of nanocrystalline TiO_2 co-sensitised by novel cyanine dyes. *Solar Energy Materials and Solar Cells*, 88(1), 23-35.
9. Ehret, A.; Stuhi, L.; and Spitler, M.T. (2001). Spectral sensitisation of TiO_2 nanocrystalline electrodes with aggregated cyanine dyes. *Journal of Physical Chemistry B*, 105(41), 9960-9965.
10. He, J.; Lindström, H.; Hagfeldt, A.; and Lindquist, S.E. (2000). Dye-sensitised nanostructured tandem cell-first demonstrated cell with a dye-sensitised photocathode. *Solar Energy Materials and Solar Cells*, 62(3), 265-275.

11. Inakazu, F.; Noma, Y.; Ogomi, Y.; and Hayase, S. (2008). Dye-sensitised solar cells consisting of dye-bilayer structure stained with two dyes for harvesting light of wide range of wavelength. *Applied Physics Letters*, 93, 093304.
12. Ogomi, Y.; Pandey, S.S.; Kimura, S.; and Hayase, S. (2010). Probing mechanism of dye double layer formation from dye-cocktail solution for dye-sensitised solar cells. *Thin Solid Films*, 519(3), 1087-1092.
13. Noma, Y.; Iizuka, K.; Ogomi, Y.; Pandey, S.S. and Hayase, S. (2009). Preparation of double dye layer structure of dye-sensitised solar cells from cocktail solution for harvesting light in wide range of wavelengths. *Japanese Journal of Applied Physics*, 48, 020213.
14. Pham, W.; Lai, W.F.; Weissleder, R.; and Tung, C.H. (2003). High efficiency synthesis of a bioconjugatable near-infrared fluorochrome. *Bioconjugate Chemistry*, 14(5), 1048-1051.
15. Pandey, S.S.; Inoue, T.; Fujikawa, N.; Yamaguchi, Y.; and Hayase, S. (2010). Substituent effect in direct ring functionalized squaraine dyes on near infra-red sensitisation of nanocrystalline TiO_2 for molecular photovoltaics. *Journal of Photochemistry and Photobiology A*, 214(2-3), 269-275.
16. Frisch, M.J.; Trucks, G.W.; Schlegel, H.B.; Scuseria, G.E.; Robb, M.A.; Cheeseman, J.R.; Scalmani, G.; Barone, V.; Mennucci, B.; Petersson, G.A.; Nakatsuji, H.; Caricato, M.; Li, X.; Hratchian, H.P.; Izmaylov, A.F.; Bloino, J.; Zheng, G.; Sonnenberg, J.L.; Hada, M.; Ehara, M.; Toyota, K.; Fukuda, R.; Hasegawa, J.; Ishida, M.; Nakajima, T.; Honda, T.; Kitao, O.; Nakai, H.; Vreven, T.; Peralta, Jr.J.E.; Ogliaro, F.; Bearpark, M.; Heyd, J.J.; Brothers, E.; Kudin, K.N.; Staroverov, V.N.; Kobayashi, R.; Normand, J.; Raghavachari, K.; Rendell, A.; Burant, J.C.; Iyengar, S.S.; Tomasi, J.; Cossi, M.; Rega, N.; Millam, J.M.; Klene, M.; Knox, J.E.; Cross, J.B.; Bakken, V.; Adamo, C.; Jaramillo, J.; Gomperts, R.; Stratmann, R.E.; Yazyev, O.; Austin, A.J.; Cammi, R.; Pomelli, C.; Ochterski, J.W.; Martin, R.L.; Morokuma, K.; Zakrzewski, V.G.; Voth, G.A.; Salvador, P.; Dannenberg, J.J.; Dapprich, S.; Daniels, A.D.; Farkas.; Foresman, J.B.; Ortiz, J.V.; Cioslowski, J.; Fox, D.J. (2009). *Gaussian 09, Revision A.02*, Gaussian Inc., Wallingford CT.
17. Tomasi, J.; Mennucci, B.; and Cammy, R. (2005). Quantum mechanical continuum solvation models. *Chemical Reviews*, 105, 2999-3093.
18. Fantacci, S.; Angelis, D.F.; Wang, J.J.; Bernhard, S.; and Selloni, A. (2004). A combined computational and experimental study of polynuclear Ru-TPPZ complexes: Insight in to the electronic and optical properties of coordination polymers. *Journal of American Chemical Society,* 126(31), 9715-9723.
19. de Miguel, G.; Marchena, M.; Ziółek, M.; Pandey, S.S.; Hayase, S.; and Douhal, A. (2012). A femto to millisecond photophysical characterisation of indole-based squaraines adsorbed on TiO_2 nanoparticles. *Journal of Physical Chemistry C,* 116(22), 12137-12148.
20. Yum, J.H.; Moon, S.J.; Baker, R.H.; Walter, P.; Geiger, T.; Nüesch, F.; Gratzel, M.; and Nazeeruddin, M.K. (2008). Effect of co-adsorbent on the photovoltaic performance of squaraine sensitised nanocrystalline solar cells. *Nanotechnology*, 42(19), 424005.
21. Hagfeldt, A.; and Gratzel, M. (1995). Light induced redox reactions in nanocrystalline systems. *Chemical Reviews*, 95(1), 49-68.

22. Ogomi, Y.; Kato, T.; and Hayase, S. (2006). Dye sensitised solar cells consisting of ionic liquids and solidification. *Journal of Photopolymer Science and Technology*, 19, 403-408.
23. Pandey, S.S.; Inoue, T.; Fujikawa, N.; Yamaguchi, Y.; and Hayase, S. (2010). Alkyl and fluoroalkyl substituted squarine dyes: a prospective approach towards development of novel NIR sensitisers. *Thin Solid Films*, 519(3), 1066-1071.
24. Nazeeruddin, M.K.; Pechy, P.; Renouard, T.; Nazeeruddin, S.K.; Robin-Humphrey, B.; Comte, P.; Cevey, L.; Costa, E.; Shklover, V.; Spiccia, L.; Liska, P.; Deacon, G.B.; Bignozzi, C.A.; and Gratzel, M. (2001). Engineering of efficient panchromatic sensitisers for nanocrystalline TiO2-Based solar cells. *Journal of American Chemical Society*, 123(8), 1613-1624.
25. Guillemoles, J.F.; Barone, V.; Joubert, L.; and Adamo, C.A. (2002). Theoretical investigations of the ground and excited states of selected Ru and Os polypyridyl molecular dyes. *Journal of Physical Chemistry A*, 106, 11354-11360.
26. Lee, C.; Yang, W.; and Parr, R.G. (1988). Development of the Colic-Salvetti correlation-energy formula into a functional of the electron density. *Physical Review B*, 37(2), 785-789.
27. Pastore, M.; Mosconi, E.; Angelis, D.F.; and Gratzel, M. (2010). A computational investigation of organic dyes for dye-sensitised solar cells: benchmark, strategies, and open issues. *Journal of Physical Chemistry C*, 114(15), 7205-7212.
28. Vosko, S.H.; Wilk, L.; Nusair, M. (1980). Accurate spin-dependent electron liquid correlation energies for local spin density calculations: a critical analysis. Canadian Journal of Physics, 58(8), 1200-1211.